# Quantum Scattering of Distinguishable Bosons using an Ultracold Atom Collider

Angela S. Mellish,[1] Niels Kjærgaard,[1,2,3] Paul S. Julienne,[4] and Andrew C. Wilson[1]

[1]*Department of Physics, University of Otago, Dunedin, New Zealand*
[2]*Niels Bohr Institute, University of Copenhagen, Denmark*
[3]*QUANTOP—Danish National Research Foundation Center for Quantum Optics*
[4] *National Institute of Standards and Technology, 100 Bureau Drive,*
*Stop 8423, Gaithersburg, Maryland, 20899-8423 USA*
(Dated: February 6, 2008)

We describe a new implementation of magnetic collider for investigating cold collisions between ultracold atomic clouds in different spin states, and we use this to investigate scattering involving both even and odd order partial waves. Our method relies on the axial assymetry of a double-well magnetic trap to selectively prepare the spin state in each cloud. We measure the energy dependence of $s$, $p$ and $d$ partial wave phase shifts in collisions up to 300 $\mu$K between $^{87}$Rb atoms in the $5S_{1/2}, F = 1, m_F = -1$ and $5S_{1/2}, F = 2, m_F = 1$ states.

Collisions in ultracold and degenerate quantum gases play a key role in many of their interesting properties [1]. So far, investigations with ultracold atoms have been mostly concerned with *s*-wave scattering processes, but now nonzero partial waves play a critical role in many investigations, (see, e.g., [2]). A magnetic collider scheme for determining the contribution made by higher-order partial waves was recently implemented [3, 4]. In these experiments the atoms were in the same spin state, limiting the collisions to those involving only even-order partial waves — a consequence of the particles being indistinguishable bosonic particles.

In the present work, we extend our collider method to *distinguishable* bosons for which the scattering is fundamentally different since both odd and even angular momentum components are allowed. As in our original work [3], spin-polarized $^{87}$Rb atoms are loaded into a magnetic double-well potential which is then transformed to a single well to initiate a collision. Here, however, one of the clouds is converted to a different spin state prior to collision making the scattering

patterns crucially different. We observe the interference of $s$, $p$ and $d$ partial waves for collisions between atoms in the $F = 1, m_F = -1$ and $F = 2, m_F = 1$ hyperfine ground states. Despite the complexity of the three-wave interference, we successfully determine the three partial wave phase shifts for energies up to 300 $\mu K$ as measured in units of the Boltzmann constant $k_B$.

The angular dependence of the two-body scattering problem is described by the complex scattering amplitude $f(\theta)$ [6]. Using the partial wave expansion, this is expressed as $f(\theta) = \frac{1}{2ik} \sum_{\ell=0}^{\infty} (2\ell + 1)(e^{2i\eta_\ell} - 1)P_\ell(\cos\theta)$, where $P_\ell$ is the $\ell^{\text{th}}$ order Legendre polynomial and $\eta_\ell$ are the partial wave phase shifts which depend on the scattering potential and relative wave vector $k$ of the colliding atom pair. For the range of energies we focus on here, only the first three partial waves $\ell = 0, 1, 2$ contribute [7]. In this case the differential cross-section $d\sigma/d\Omega = |f(\theta)|^2$ is given by

$$
\begin{aligned}
\frac{\mathrm{d}\sigma}{\mathrm{d}\Omega} &= \frac{1}{k^2}\{\sin^2\eta_0 + 9\sin^2\eta_1\cos^2\theta + \frac{25}{4}\sin^2\eta_2(3\cos^2\theta - 1)^2 + 6\sin\eta_0\sin\eta_1\cos(\eta_0 - \eta_1)\cos\theta \\
&+ 5\sin\eta_0\sin\eta_2\cos(\eta_0 - \eta_2)(3\cos^2\theta - 1) + 15\sin\eta_1\sin\eta_2\cos(\eta_1 - \eta_2)(3\cos^2\theta - 1)\cos\theta\}.
\end{aligned}
\tag{1}
$$

Because of the orthogonality and completeness of the Legendre polynomials, a fit of an interference expression in the form Eq. (1) to a measured angular distribution directly gives the partial wave phase shifts $\eta_0$, $\eta_1$ and $\eta_2$ irrespective of knowledge about absolute quantities such as particle flux [4].

Our experimental procedure is as follows. $^{87}$Rb atoms in the $5S_{1/2}F = 1, m_F = -1$ ($\equiv |1\rangle$) state are loaded into a magnetic quadrupole-Ioffe-configuration (QUIC) trap [8] with trap frequencies $\omega_z/2\pi = 11$ Hz axially and $\omega_\rho/2\pi = 90$ Hz radially. The details of loading the double-well trap and initiating a collision are much the same as described in [3]. In summary, after rf-induced evaporation of the atoms to a tem-

perature of approximately 2 $\mu$K we adiabatically transform the potential to a double well by raising a potential barrier along the axial dimension of the trap to split the cloud in half [9]. The clouds are then further evaporatively cooled to a temperature of typically a few hundred nano-Kelvin, just above the Bose-Einstein condensation transition temperature. A collision between the clouds is initiated by rapidly transforming the potential back to a single well. The collision energy is selected by adjusting the well spacing in the double-well trap.

To enable a collision between atoms in different spin states, we apply a two-photon pulse consisting of a microwave ($\sim$ 6.8 GHz) and an rf ($\sim$ 2 MHz) photon (depending on the Zee-
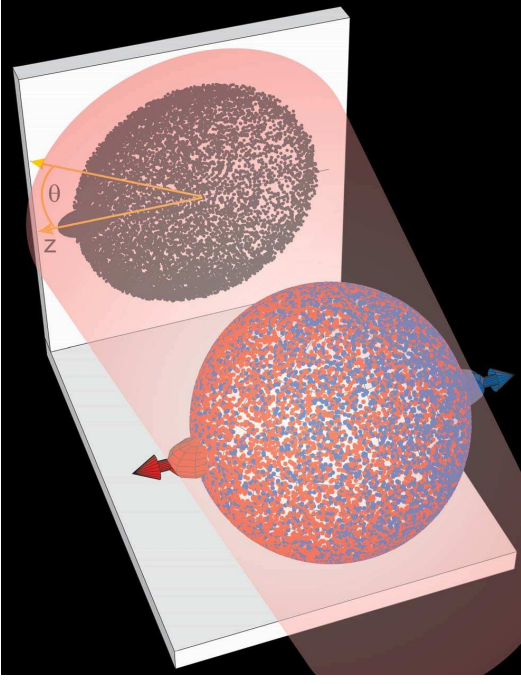
FIG. 1: (color online) After a collision between two atomic clouds in different spin states, pairs of diametrically-opposite scattered particles will be distributed over the expanding Newton sphere according to the differential cross-section. Using a light beam resonant with only one of the states (depicted as red), an absorption image of the contribution of this particular state to the scattering halo is obtained.



FIG. 2: (color online) Scattering images for a collision at $E/k_B = 135$ $\mu$K, (a) probing only atoms in the $F = 2$ state and (b) probing both the $F = 1$ and $F = 2$ states. The asymmetry in the scattering pattern of (a) is due to $p$-wave scattering. The corresponding angular scattering probability is shown in (c) with a fit to Eq. (1) (solid line).

man splitting) to transfer $|1\rangle$ state atoms to the $5S_{1/2}, F = 2, m_F = 1 (\equiv |2\rangle)$ state [10]. Due to the intrinsic axial asymmetry of the QUIC trap the clouds are situated at slightly different magnetic field values immediately after the double- to single-well trap transformation. This enables us to selectively address and convert up to 90 % of the atoms in one of the clouds, while only 10 % of the atoms in the other cloud are converted to the $|2\rangle$ state. To first order, the $|1\rangle$ and $|2\rangle$ states have the same magnetic moment and experience the same confinement potential.

To selectively probe the scattered $|2\rangle$ state atoms we apply a 20 $\mu$s pulse of resonant light on the $5S_{1/2}, F = 2 \rightarrow 5P_{3/2}, F' = 3$ transition along a radial direction shortly after the end of the collision, and acquire an absorption image. This leaves the $|1\rangle$ state atoms undetected. An illustration of this is shown in Fig. 1. Alternatively, we can simultaneously probe both the $|1\rangle$ and $|2\rangle$ state atoms by applying some $5S_{1/2}, F = 1 \rightarrow 5P_{3/2}, F' = 2$ light to pump all of the atoms to the $F = 2$ level shortly before the probing pulse.

Figure 2 shows absorption images after a collision at $E/k_B = 135$ $\mu$K between atomic clouds in the $|1\rangle$ and $|2\rangle$ states. In Fig. 2(a) only atoms in the $|2\rangle$ state have been probed, whereas in (b) atoms in both the $|1\rangle$ and $|2\rangle$ states are imaged. The distinct left-right asymmetry of the scattered atoms in (a) is the result of partial-wave interference between the odd ($\ell = 1$) $p$-wave and even $s$- and $d$-waves. The scattering amplitude of the $p$-wave component changes sign at $\theta = \pm\pi/2$ as can be seen in Fig. 3. For the collision
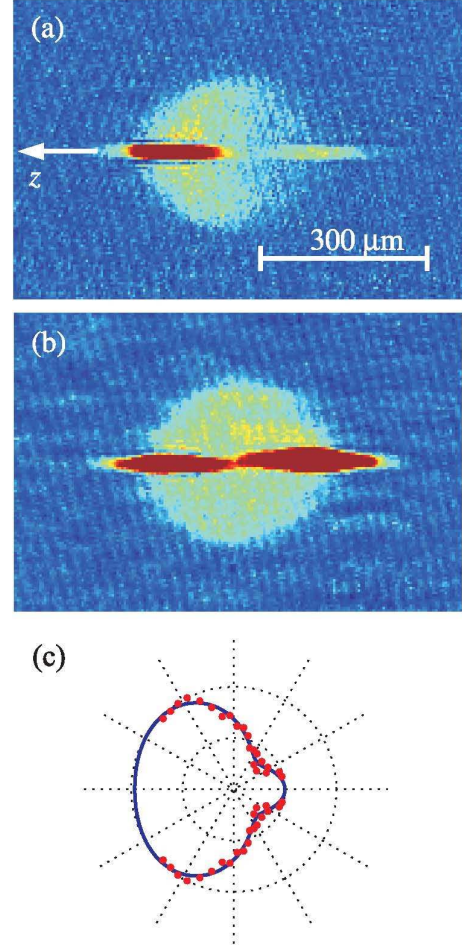
energy in this example, where the $d$-wave contribution is relatively small, the $p$-wave interferes constructively with $s$-wave for angles $|\theta| < \pi/2$ and destructively for $|\theta| > \pi/2$ where $\theta$ is defined with respect to the collision axis in the initial direction of travel (i.e., for the $|2\rangle$ state shown in Fig. 2, $|\theta| < \pi/2$ is to the left of the image). Since $\theta$ is defined with the opposite sense for the $|1\rangle$ and $|2\rangle$ states, $f(\theta)$ for the $|1\rangle$ state is complementary to that of $|2\rangle$ and imaging both states together results in a symmetric scattering pattern [Fig. 2(b)].

We analyze the absorption images of the scattering patterns using the method described in [11]. Briefly, we reconstruct the 3D distribution of the scattered atoms using the inverse Abel transformation [12]. The Abel-inverted image is divided into 30 angular bins which reflect the trajectories of scattered atoms in the harmonic potential. The number of scattered particles in each of the bins yields a measure of the angular scattering probability, which is proportional to the differential cross-section in Eq. (1). We fit Eq. (1) to this data to obtain the partial wave phase shifts $\eta_0$, $\eta_1$ and $\eta_2$ for the $s$, $p$, and
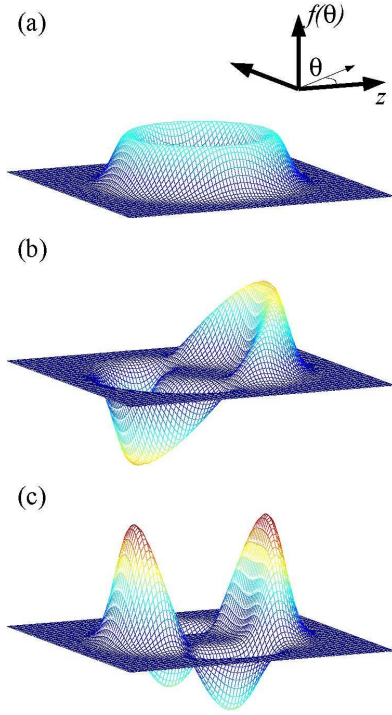
FIG. 3: (color online) A graphical representation of the contributions to the scattering amplitude for the first three partial waves; (a) $s$-wave, (b) $p$-wave and (c) $d$-wave. The sign and magnitude of each $\ell$ term in $f(\theta)$ is plotted vertically for a spherical scattering shell with a Gaussian profile in the radial direction. The relative scale of each is determined by $\eta_\ell$. In contrast to $s$- and $d$-wave, the $p$-wave contribution to $f(\theta)$ is antisymmetric in $\theta$.
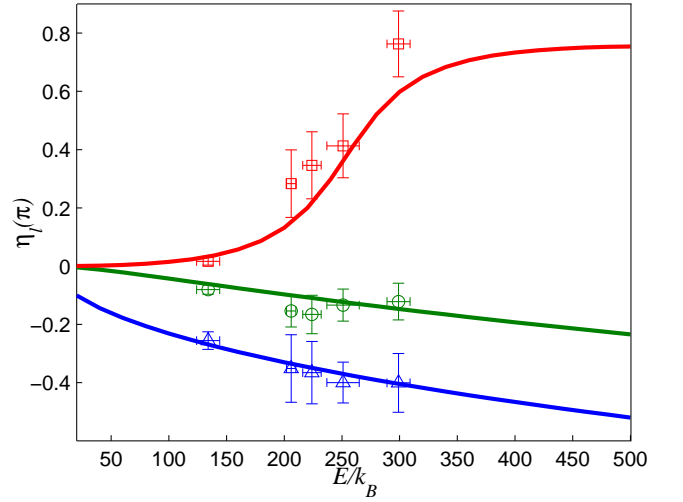


FIG. 4: (color online) The partial wave phase shifts for collisions between the $|1\rangle$ and $|2\rangle$ states. The symbols represent the $s$ ($\triangle$), $p$ ($\bigcirc$) and $d$ ($\square$) phase shifts extracted from the data and the solid lines are a theoretical calculation from a coupled-channels model.

$d$ partial waves respectively. As emphasized by Buggle *et al.* [4], this is an interferometric method which does not rely on absolute particle numbers and identifies only the amplitudes and relative signs of the phase shifts. The $s$-wave scattering length is known to be positive (repulsive interaction) for the states considered here so we choose the corresponding solution where $\eta_0 < 0$ for our energy range. The collision energy $E = mv_{\rm rel}^2/4 = \hbar k^2/m$ is measured within a typical uncertainty of $5\ \mu K$ by determining the relative velocity $v_{\rm rel}$ from a linear fit to the position of the clouds over approximately 2 ms either side of collision. In Fig. 4 each phase shift value is the average of up to 10 measurements at the particular collision energy. The error bars on the data combine statistical uncertainty and errors associated with the fit to Eq. (1).

A comparison of the measurements to theoretical predictions is shown in Fig. 4. These are standard coupled-channels numerical calculations [13, 14, 15] for the collision of two atoms in hyperfine states $F, M$ and $F', M'$ in a low magnetic field $B$ with relative (partial wave) angular momentum $\ell$ and projection $m$. All channels $\{FM, F'M', \ell m\}$ coupled by terms in the molecular Hamiltonian are included. Only channels with $M_{\rm tot} = M + M' + m$ can couple to one another and because the collisions are from a single direction (defined by the vector connecting the two initial separated atomic clouds) we need only include the $M_{\rm tot} = 0$

channels. The Hamiltonian contains the radial $T_R$ and rotational $T_{\rm rot}$ kinetic energy terms, the electron-electron spin-spin interaction $\alpha^2 H_{\rm ss}$ (where $\alpha$ is the fine structure constant), the electron-nuclear spin interaction terms $\alpha^2 H_{\rm hf}$ that gives the atomic hyperfine energies, and the strong chemical interactions described by the two adiabatic Born-Oppenheimer potential curves that correlate with two separated $^2$S atoms. These potential curves correspond to the electronic states of $^1\Sigma_g^+$ and $^3\Sigma_u^+$ symmetry. There are 8 $s$-wave channels needed to describe $M_{\rm tot} = 0$ $s$-wave collisions of $|2\rangle$ and $|1\rangle$ atoms (5 open and 3 closed). There are also 18 $M_{\rm tot} = 0$ $p$-wave collision channels (11 open and 7 closed), and 30 $M_{\rm tot} = 0$ $d$-wave channels (18 open and 12 closed). All of these channels are included in the basis set for each partial wave. If the channels are designated by the index $j$, so that the wavefunction for atoms in the entrance channel $i$ is $\Psi_i = \sum_j |j\rangle f_{ji}(R)/R$, the coupled Schrödinger equations, in a basis set defined by the separated atom quantum numbers, takes on the form

$$\frac{\hbar^2}{2\mu}\frac{d^2 f_{ki}}{dR^2} + \left(E - E_k - \frac{\hbar^2 \ell_k(\ell_k+1)}{2\mu R^2}\right) f_{ki}(R)$$
$$- \sum_j V_{kj}(R) f_{ji}(R) = 0. \qquad (2)$$

Here $E_k$ and $\ell_k$ are the respective Zeeman energy and relative angular momentum quantum number of the two colliding separated atoms for the magnetic field $B$, and the potential matrix elements $V_{kj}$ define the interchannel coupling. These equations are solved numerically using standard algorithms [16]. For comparison with the data, the calculation uses a magnetic field of 0.23 mT, and the scattering potentials are characterized by a dispersion coefficient $C_6 = 4703$ au and triplet $a_t = +98.96\ a_0$ and singlet $a_s = +90.1\ a_0$ scattering lengths consistent with [17] (1 au $= E_h a_0^6$, where $E_h = 4.36 \times 10^{-18}$ J and $a_0 = 0.0529$ nm).

As can be seen in Fig. 4, our experimental observations are described well by the theoretical model. The dramatic change of the $d$-wave phase shift is a signature for the $d$-wave shape resonance known to occur for collisions between two $^{87}$Rb atoms [3, 4, 18]. We estimate the position of the resonance to be $(235 \pm 50)$ $\mu$K with a width of approximately 120 $\mu$K (FWHM) from a Lorentzian fit to the data around the resonance. Calculated inelastic collision rate constants remain below $10^{-13}$ cm$^3$/s over the collision range of interest (compared to a maximum total elastic scattering cross-section of $\sim 1.6 \times 10^{-11}$ cm$^2$), even when enhanced by the $d$-wave shape resonance. This is due to the exceptional case that both potentials have similar scattering phase shifts at low collision energies for threshold $^{87}$Rb spin-exchange relaxation [19, 20, 21]. Correspondingly, we do not observe any atom loss from the trap resulting from the collision.

Two effects are not included in our analysis: state impurities in the clouds and the possibility of multiple scattering. The first of these is a difficult technical issue relating to our set-up and the second is of a more fundamental nature. With state impurities in both clouds, the collision processes which can occur are $|1\rangle + |2\rangle$, $|2\rangle + |2\rangle$, $|1\rangle + |1\rangle$, and $|2\rangle + |1\rangle$, with relative amounts depending on the density of impurities. If these effects were significant one would expect the presence of collisions between the $|1\rangle$ and $|2\rangle$ states in the "wrong" direction to diminish the measured $p$-wave contribution, whereas scattering due to the $|2\rangle + |2\rangle$ and $|1\rangle + |1\rangle$ collision processes would increase the perceived $s$- and $d$-wave phase shifts measured which is clearly not the case in Fig. 4. As for the second issue, we observe only approximately one-third of the total number of atoms scattered after a collision near the resonance, indicating that the probability of a secondary collision is relatively small. A detailed theoretical analysis of multiple scattering is difficult outside the $s$-wave regime, and particularly near a $d$-wave shape resonance, since the energy and centre-of-mass of a subsequent collision depend crucially on the scattering angle after the first collision.

In conclusion, we have investigated the energy dependence of collisions between two $^{87}$Rb clouds in different spin states. Our experimental observations agree well with predictions from a theoretical coupled-channels model. We note that the collision between two such particles of different spins provides a mechanism for producing spin entanglement. The resulting pair correlation could potentially be observed as in recent experiments on dissociating molecules [22] and colliding Bose-Einstein condensates [23]. Furthermore, the occurrence of a $d$-wave resonance and the resulting directionality of scattered particles may serve as a vehicle for the production of pair correlated beams.

[1] K. Burnett, P. S. Julienne, P. D. Lett, E. Tiesinga, and C. J. Williams, Nature **416**, 225 (2002); J. Weiner, *Cold and Ultra-cold Collisions in Quantum Microscopic and Mesoscopic Systems* (Cambridge University Press, 2003).

[2] C. A. Regal, C. Ticknor, J. L. Bohn, and D. S. Jin, Phys. Rev. Lett. **90**, 053201 (2003); C. Ticknor, C. A. Regal, D. S. Jin, and J. L. Bohn, Phys. Rev. A **69**, 042712 (2004); K. Günter, T. Stöferle, H. Moritz, M. Köhl, and T. Esslinger, Phys. Rev. Lett. **95**, 230401 (2005); F. Chevy *et al.*, Phys. Rev. A **71**, 062710 (2005); T. Volz, S. Dürr, N. Syassen, G. Rempe, E. van Kempen, and S. Kokkelmans, *ibid.* **72**, 010704(R) (2005); M. Anderlini and D. Guéry-Odelin, *ibid.* **73**, 032706 (2006); R. V. Krems, Phys. Rev. Lett. **96**, 123202 (2006).

[3] N. R. Thomas, N. Kjærgaard, P. S. Julienne, and A. C. Wilson, Phys. Rev. Lett. **93**, 173201 (2004).

[4] Ch. Buggle, J. Léonard, W. von Klitzing, and J. T. M. Walraven, Phys. Rev. Lett. **93**, 173202 (2004).

[5] Observation of $s + p$ partial wave interference in cold collisions has previously been reported in R. Legere and K. Gibble, Phys. Rev. Lett. **81**, 005780 (1998).

[6] J. R. Taylor, *Scattering Theory* (Wiley, New York, 1972).

[7] Calculations show that contributions from higher partial wave are negligible, e.g., $\eta_4 < 0.02 \times \pi$ for collision energies up to 500 $\mu$K.

[8] T. Esslinger, I. Bloch, and T. W. Hänsch, Phys. Rev. A **58**, R2664 (1998).

[9] N. R. Thomas, A. C. Wilson, and C. J. Foot, Phys. Rev. A **65**, 063406 (2002).

[10] M. R. Matthews *et al.*, Phys. Rev. Lett. **81**, 243 (1998).

[11] N. Kjærgaard, A. S. Mellish, and A. C. Wilson, New J. Phys. **6**, 146 (2004).

[12] V. Dribinski, A. Ossadtchi, V. A. Mandelshtam, and H. Reisler, Rev. Sci. Instrum. **73**, 2634 (2002).

[13] H. T. C. Stoof, J. M. V. A. Koelman, and B. J. Verhaar, Phys. Rev. B **38**, 4688 (1988).

[14] F. H. Mies, C. J. Williams, P. S. Julienne, and M. Krauss, J. Res. NIST **101**, 521 (1996).

[15] P. S. Julienne, in *Scattering: Scattering and Inverse Scattering in Pure and Applied Science*, edited by R. Pike and P. Sabatier (Academic Press, 2002), chap. 2.6.3, p. 1043.

[16] J. Gordon, J. Chem. Phys. **51**, 14 (1969).

[17] E. G. M. van Kempen, S. J. J. M. F. Kokkelmans, D. J. Heinzen, and B. J. Verhaar, Phys. Rev. Lett. **88**, 093201 (2002).

[18] H. M. J. M. Boesten, C. C. Tsai, J. R. Gardner, D. J. Heinzen, and B. J. Verhaar, Phys. Rev. A **55**, 636 (1997).

[19] J. P. Burke, Jr., J. L. Bohn, B. D. Esry, and C. H. Greene, Phys. Rev. A **55**, R2511 (1997).

[20] P. S. Julienne, F. H. Mies, E. Tiesinga, and C. J. Williams, Phys. Rev. Lett. **78**, 1880 (1997).

[21] S. J. J. M. F. Kokkelmans, H. M. J. M. Boesten, and B. J. Verhaar, Phys. Rev. A **55**, R1589 (1997).

[22] M. Greiner, C. A. Regal, J. T. Stewart, and D. S. Jin, Phys. Rev. Lett. **94**, 110401 (2005).

[23] C. I. Westbrook *et al.*, quant-ph/0609019.